Comprehensive Analysis of the Autophagy-Dependent Ferroptosis-Related Gene FANCD2 in Lung Adenocarcinoma

huikai miao
Sun Yat-sen University Cancer Center
qiannan ren
Sun Yat-sen University Cancer Center
hongmu li
Sun Yat-sen University Cancer Center
mingyue zeng
Sun Yat-sen University Cancer Center
dongni chen
Sun Yat-sen University Cancer Center
youfang chen
Sun Yat-sen University Cancer Center
zhesheng wen (wenzhsh@sysucc.org.cn)
Sun Yat-sen University Cancer Center

Research

Keywords: lung adenocarcinoma, autophagy-dependent ferroptosis, FANCD2, prognosis, immunity

Posted Date: June 7th, 2021

DOI: https://doi.org/10.21203/rs.3.rs-541121/v1

Abstract

Background. The development of lung adenocarcinoma (LUAD) involves the interactions between cell proliferation and death. Autophagy-dependent ferroptosis, a distinctive cell death process was implicated in a multitude of diseases, whereas no research revealing the relationship between autophagy-dependent ferroptosis and LUAD pathogenesis was reported. Thus, the primary objective was to explore the role and potential function of the autophagy-dependent ferroptosis-related genes in LUAD.

Methods. Clinical information and transcriptome profiling of patients with LUAD were retrieved and downloaded from open-source databases. Autophagy-dependent ferroptosis-related genes were screened by published articles. The key gene was identified as the intersection between the differentially expressed genes and prognosis-related genes. Patients were divided into high- and low-risk groups using the expression level of the key gene. The validity of the key gene prognosis model was verified by survival analysis. The correlation between the clinical characteristics of LUAD and the expression level of the key gene was analyzed to explore the clinical significance and prognosis value. And the roles of the key gene in response to chemotherapy, immune microenvironment and tumor mutation burden were predicted. The validation of key gene expression levels were further performed by immunohistochemistry staining.

Results. FANCD2, a key autophagy-dependent ferroptosis-related gene by searching database, was confirmed as an independent prognostic factor for LUAD occurrence. The high expression level of FANCD2 was associated with an advantaged TNM stage, a less chemotherapy sensitivity, a low ImmuneScore, which indicated a deactivation status in immune microenvironment, a high tumor mutation burden, and a poor survival for LUAD patients. Pathway enrichment analysis showed that FANCD2 were involved in response to oxidative stress and neutrophil mediated immunity. Immunohistochemistry staining showed that the expression level of FANCD2 is higher in LUAD patients than normal tissue samples, which was in accordance with the database report.

Conclusion. FANCD2, a key gene related to autophagy-dependent ferroptosis, could work as a biomarker, which predicts the survival, chemotherapy sensitivity, tumor immunity and mutation burden of LUAD. Research of autophagy-dependent ferroptosis and targeting the FANCD2 may offer a new perspective for the treatment and improvement of prognosis in LUAD.

Introduction

Lung adenocarcinoma (LUAD) is one of the most common malignant tumors in the world, demonstrating a rising trend in recent years [1]. Traditional treatments, such as surgery, radiotherapy, and chemotherapy, could not meet all LUAD patients' needs due to the high recurrence and metastasis. Although immunotherapy has been shown to improve survival in LUAD patients, the 5-year overall survival rate is only 23% [2]. The pathogenic mechanism of LUAD should be further elucidated to discover a new effective treatment strategy.

The tumor heterogeneity, including immune microenvironment and tumor mutation burden, could affect the immunotherapy effectiveness. The recent research has revealed that ferroptosis is also involved in T cell immunity and cancer immunotherapy. The increased ferroptosis contributes to the anti-tumour efficacy of immunotherapy [3].

Ferroptosis is an iron-dependent form of regulated cell death which is characterized by the excess reactive oxygen species (ROS) generation and lethal accumulation of lipid peroxidation [4] [5] [6]. Disregulation of ferroptosis has been implicated in multiple physiological and pathological processes, including cancer cell death and T-cell immunity [7]. Autophagy-dependent ferroptosis is a key type of ferroptosis which is featured by excessive autophagy and lysosome activity [8]. The influence of ferroptosis, especially autophagy-dependent ferroptosis, on tumor microenvironment needs to be further studied.

The iron metabolism and homeostasis could be influenced by immune cells and related molecules [9]. Immune cells in the microenvironment play crucial roles in the maintenance of iron metabolism balance [10]. The excessive activation of ferroptosis in tumor cells can lead to tumor antigens exposure which activates the immnue system. Then, the immunogenicity of the microenvironment was improved and the effectiveness of immunotherapy was enhanced [11]. Immunotherapy can activate CD8 + T cells to enhance the lipid peroxidation in tumor cells, which further contribute to the increase in ferroptosis in turn [3]. Therefore, targeting ferroptosis to improve the effectiveness of cancer immunotherapy might become a prospective strategy in the future. In the clinical applications of immunotherapy, tumor mutation burden (TMB) is emphasized as an emerging feature and a biomarker of immunotherapy response [12] [13]. TMB is defined as the total number of somatic, coding, base substitution, and indel mutations per megabase of genome examined [14]. Each of these mutations results in the generation of one protein that is an new antigen and could be recognized by the immune system [15]. Highly mutated tumors are more likely to carry neoantigens, making them become the targets for activated immune cells [14].

In this study, we comprehensively analyze the genome of LUAD, identify autophagy-dependent ferroptosis-related genes closely associated with the prognosis and chemotherapy sensitivity, further construct and validate the predictive model of the key gene, and explore the relationship with immune infiltration and tumor mutation. Our findings may help generate personalized treatment and improve the clinical outcomes of LUAD patients.

Materials And Methods

Workflow

A multi-step approach was used to identify and analyse the autophagy-dependent ferroptosis-related key gene in LUAD. The transcriptome and clinical information were downloaded from The Cancer Genome Atlas (TCGA) project and Gene Expression Omnibus (GEO) data. Autophagy-dependent ferroptosis-related genes were screened by the published articles. Differentially expressed genes (DEGs) related to autophagy-dependent ferroptosis were identified. Univariate and multivariate Cox analyses were applied

to screen out the independent prognosis genes related to overall survival (OS). The key gene was identified by the intersection of the DEGs and the prognostic genes. The LUAD patients were classified into the high-risk and low-risk groups based on the key gene expression level. Kaplan-Meier (K-M) analysis and receiver operating characteristic (ROC) curve were conducted to analyze the survival prognosis of patients in TCGA and GEO cohort. Chemotherapy sensitivity was predicted between different risk group. Gene ontology (GO) and Kyoto encyclopedia of genes and genomes (KEGG) were conducted to investigate the potential bio-function of the key gene. ImmuneScore was calculated using the Tumor Immune Estimation Resource (TIMER) algorithm and the TMB was counted as the total number of mutations per megabyte of tumor tissue.

LUAD patients dataset processing

All the RNA-Seq data was normalized as fragments per kilobase of transcript per million mapped reads. mRNAs ensemble gene identities were derived from the HUGO Gene Nomenclature Committee (HGNC) database. The corresponding clinical information include age, gender, tumor grade, lymph node metastasis, AJCC TNM stages and survival outcomes. Patients with insufficient clinical data were excluded. OS was estimated as the primary endpoint.

Construction and validation of an autophagy-dependent ferroptosis-related gene signature

Autophagy-dependent ferroptosis-related genes were retrieved from the literatures published before January 2021. The gene expression file was obtained after combining the related mRNA expression and the clinical data. The DEGs between tumor and normal tissues were identified with a false discovery rate (FDR) < 0.05 in the TCGA cohort. Univariate and multivariate Cox analysis of OS were performed to screen the genes with prognostic values. The key gene was identified by the intersection of the DEGs and the prognostic genes in the TCGA cohort. Patients were stratified into high-risk and low-risk groups based on the median value of the key gene expression. And the prognostic value was validated by a GEO cohort (GSE116959). The clinical correlation analysis of the key gene was conducted between high- and low-risk groups.The time-dependent ROC curve analyses were conduct to evaluate the predictive power of the key gene. The mRNA expression level of the key gene in various types of cancers were identified in the Oncomine database [16]. The mRNA and protein expression of the key gene in LUAD were determined using the Gene Expression Profiling Interactive Analysis (GEPIA) and The Human Protein Atlas (HPA) database [17] [18].

Chemotherapeutic response prediction

The commonly used chemotherapy for lung adenocarcinoma, including pemetrexed, cisplatin, gemcitabine, paclitaxel, vinorelbine, docetaxel, doxorubicin, etoposide, erlotinib and gefitinib, were all analyzed in our study [19]. The chemotherapeutic response was estimated by using the R package “pRRophetic” [20]. The half maximal inhibitory concentration (IC50) of each patients of different risk group were compared.

Functional enrichment analysis

The biological functions and pathways of the key gene were elucidated through the DEGs between the high-risk and low-risk groups. GO enrichment and KEGG pathway analyses were then were assessed in DAVID database.

Correlation between the key gene and tumor immune cell infiltration

The enrichment levels of immune cells was quantified by the Tumor Purity, Estimate Score, Immune Score and Stromal Score in each sample. The tumor immune cell infiltration was calculated by Single Sample Gene Set Enrichment Analysis (ssGSEA). Then we analyzed the correlation between the key gene expression and the abundance of infiltrating immune cells (B cells, CD8+ T cells, CD4+ T cells, macrophages, neutrophils and dendritic cells) via The Tumor IMmune Estimation Resource (TIMER) database [21].

Analyses of somatic mutations and TMB estimation

The somatic mutation profiles of LUAD patients were downloaded from TCGA database. The mutation frequency with number of variants/the length of exons (38 million) were calculated for each sample. The OncoPlot of the top 10 mutated genes were plotted. The detailed mutational information, including the variant classification, the number of variant type and the single-nucleotide variant (SNV) class were displayed. Then we assessed the corelation between the key gene expression and the TMB levels.

Preparation of LUAD and normal tissue samples and immunohistochemistry

The clinical tissue samples of LUAD were obtained from patients who received surgery in Thoracic Oncology Department of Sun Yat-sen University Cancer Center, which was approved by the Institutional Review Committee of Sun Yat-sen University Cancer Center. The protein expression of the key gene in LUAD were determined using immunohistochemistry. The detail immunohistochemistry procedure was performed according to strict adherence to the manufacturers' instructions. LUAD samples were fixed using 10% formalin and were embedded in paraffin. Immunohistochemistry was carried out using the processed 5μm continuous sections. Samples were dewaxed with decreasing concentrations 100%, 95%, 75% and 50% of ethanol and were washed in deionized water. The sections were heated in a microwave with TE buffer pH 9.0 to retrieve antigens. Endogenous peroxidase was inhibited by incubation in goat serum. Then they were incubated in rabbit anti-FANCD2 (Proteintech, 204006-1-AP, 1:1,200) overnight at 4℃. Next, the sections were incubation with horseradish peroxidase-coupled goat anti-rabbit secondary antibody and stained using DAB Detection Kit (Polymer). The following process is cell nucleus staining, dehydration, xylene infusion, and mounting [22].

Results

Characteristics of the LUAD patients from datasets

The flow chart of this study was shown in Fig. 1. A total of 316 LUAD patients from the TCGA cohort and 381 LUAD patients from the GEO (GSE116959) cohort were finally enrolled. The detailed clinical and tumor characteristics of the LUAD cohorts were summarized in Table 1. A total of 70 autophagy-dependent ferroptosis-related genes were identified by literatures review, which was shown in Fig. 2.

Table 1
Clinical and tumor characteristics of the LUAD cohorts

	TCGA cohort	GEO cohort
No. of patients	316	381
Age (median, range)	64 (33–86)	69 (38–89)
Gender		
Female	163 (51.6%)	166 (43.6%)
Male	153 (48.4%)	215 (56.4%)
Tumor		
T 1–2	275 (87.0%)	NA
T 3–4	41 (13.0%)	NA
Node		
N 0–1	267 (84.5%)	NA
N 2–3	49 (15.5%)	NA
Metastasis		
M 0	296 (93.7%)	NA
M 1	20 (6.3%)	NA
TNM stage		
	164 (51.9%)	246 (64.6%)
	76 (24.1%)	65 (17.1%)
	56 (17.7%)	56 (14.7%)
	20 (6.3%)	14 (3.6%)
TP53		
Wide type	NA	287(75.3%)
Mutant type	NA	94(24.7%)
Survival status		
OS years (median)	2.19	2.24

LUAD, adenocarcinoma of lung, TCGA, The Cancer Genome Atlas, GEO, Gene Expression Omnibus, No: number, T: tumor, N: regional lymph node, M: metastasis, NA: not available, OS, overall survival.

Three steps were carried out to screen the key gene. First, 7 DEGs in Fig. 3A were selected. Second, 8 genes that had prognostic values for LUAD were selected (Fig. 3B). Third, the key gene was obtained as the intersection between DEGs and prognosis-related genes using Venn diagrams (Fig. 3C). As a result, FANCD2 was identified as the key gene, which worked as a prognosis-related differentially expressed gene in LUAD.

The mRNA and protein expression levels of FANCD2 were extracted by TCGA database

The FANCD2 expression in different tumors was evaluated using TCGA RNA-sequencing data (Fig. 4). FANCD2 expression was significantly higher in various tumors compared with adjacent normal tissues, and the consistent findings were shown in LUAD (Fig. 5A). After examining the mRNA expression level of FANCD2 in LUAD, the protein expression level was further explored by immunohistochemistry. There is a higher expression level of FANCD2 in LUAD tissues than normal lung tissues (Fig. 6), which is in line with the result of HPA statabase (Fig. 5B). In summary, the present results indicated that both transcriptional and translational expression levels of FANCD2 were overexpressed in patients with LUAD which may be involved in the pathogenesis of LUAD.

Prognostic risk model and predictability evaluation

The LUAD patients were stratified into high and low risk groups by the FANCD2 expression level. Table 2 showed the association of FANCD2 expression and the clinical features. A high expression of FANCD2 achieved a significant correlation with a high TNM stage (P<0.05). In the TCGA cohort, the FANCD2 expression was defined as an independent prognostic factor after the univariate and multivariate Cox regression analyses (Figure 7A). The patients in high risk groups have a poor survival than the low risk group in TCGA cohort. Similarly, relevant data from a GEO cohort (GSE35570) was used to validate the prognostic value of FANCD2 expression in LUAD (Figure 7B). Besides the poor survival and a high TNM stage, the high expression of FANCD2 was also related to a high frequency of TP53 mutation (P<0.001, Table 2). The sensitivity and specificity of the FANCD2 model was calculated by the area under ROC (TCGA cohort: AUC = 0.736, GEO cohort: AUC = 0.677), suggesting that the FANCD2 signature was effective for predicting survival of LUAD (Figure 8). We investigated the response to chemotherapy in high- and low-risk patients with LUAD, and found that 29 chemotherapeutic drugs displayed significant differences in estimated IC50 between highand low-risk patients, and that high-risk patients with LUSC showed increased sensitivity to all 29 chemotherapies (Figure 9).

Functional annotation of DEGs in different risk groups

GO and KEGG pathway enrichment analyses were used to evaluate the possible functions and pathways of the screened DEGs. As shown in Figure 10 A, the top five GO terms were response to reactive oxygen species, regulation of peptidase activity, neutrophil degranulation, neutrophil activation involved in immune response, and neutrophil activation. The top five pathways were phagosome, antigen processing and presentation, human T-cell leukemia virus, Th17 cell differentiation, and salmonella infection by KEGG enrichment (Figure 10 B).

The results of GO analysis showed that these DEGs might be involved in response to reactive oxygen species and immune processes. The data were consistent with our results that FANCD2 is correlated with ferroptosis and immune responses. Pathway enrichment analysis revealed that DEGs may be enriched in pathways related to phagosome and antigen processing and presentation, indicating that these genes function in autophagy and immune system.

Association between FANCD2 and immune-related scores

The potential immune mechanisms of LUAD were further explored through the scoring of tumor immune component (TumorPurity, ESTIMATEScore, ImmuneScore, StromalScore), and immune infiltrating cells, which all counted according to immunity-enriched groups (Figure 11). Each patient in the LUAD cohort was scored by above indicators. The immune cell infiltration levels changed along with the FANCD2 gene copy numbers (Figure 12). The LUAD patients with a high expression level of FANCD2 had a low ESTIMATEScore (Figure 12A), ImmuneScore (Figure 12B) and StromalScore (Figure 12C), but high TumorPurity (Figure 12D)was found in the high expression of FANCD2. Neutrophil cell infiltration levels seemed to positively associate with altered FANCD2 gene copy numbers in LUAD (cor = 0.15, P<0.001, Figure 13), which is consistent with the GO results of neutrophil degranulation, neutrophil activation involved in immune response, and neutrophil activation in Figure 10A.

Landscape of mutation profiles in LUAD cohort

Mutation information of LUAD cohort was displayed in oncoplot, where various colors with annotations represented the different mutation types (Figure 14). Then, the top 5 mutated genes in LUAD with ranked percentages were exhibited, including P53 (47%), TTN (41%), MUC16 (40%), RYR2 (34%) and CSMD3 (34%). These mutations were further classified according to different mutation categories. Findings indicated that missense mutation accounted for the most fraction (Figure 15A), and single nucleotide polymorphism (SNP) occurred more frequently than insertion or deletion (Figure 15B), and C>A was the most common single nucleotide variants (SNV) in LUAD (Figure 15C). The LUAD patients with a high expression level of FANCD2 showed a higher TMB (P<0.001, Figure 15D), which suggested that FANCD2 could work as a TMB marker and play a role in prediction of response to immunotherapy.

Table 2. Baseline characteristics of the patients in different risk groups

Characteristics	TCGA-LUAD cohort			GEO-LUAD cohort		
	High risk	Low risk	P value	High risk	Low risk	P value
Gender(%)			0.09			0.25
Female	71(46.4%)	88(57.1%)		112(58.9%)	103(53.9%)	
Male	82(53.6%)	66(42.9%)		78 (41.1%)	88(46.1%)	
Age (%)			0.17			0.99
< 65y	74(48.4%)	60(39.0%)		52 (27.4%)	52(27.2%)	
≥65y	79(51.6%)	94(61.0%)		138(72.6%)	139(72.8)	
TNM stage			**0.03**			**0.01**
□-□	112(73.2%)	120(77.9%)		152(80.0%)	159(83.2%)	
□-□	41(26.8)	34(22.1%)		38(20.0%)	32(16.7%)	
TP53			NA			**<0.001**
Wide type	-	-		132(69.5%)	155(81.1%)	
Mutant type	-	-		58(30.5%)	36(18.8%)	

LUAD, adenocarcinoma of lung, TCGA, The Cancer Genome Atlas, GEO, Gene Expression Omnibus, y, years, NA: not available.

Discussion

LUAD is a common malignancy with a high morbidity and mortality [1]. The development of LUAD often involves genetic abnormalities and immune dysfunction [23]. Iron metabolism could influence malignant biological behaviors and impact the tumor microenvironment [24]. The increase of labile iron in cancer cells can both facilitate DNA replication [25], and induce the coourrence of ferroptosis [4] to participate in and accelerate tumor progression.

Ferroptosis is a programmed cell death in which multiple signaling molecules interact with each other in the tumor microenvironment and synergistically regulate tumor progression [26]. Ferroptosis has a dual role in tumour promotion and suppression [27]. On the one hand, the induced tumor cell ferroptosis inhibit tumor metastases, involve in drug resistance and influence cancer immunotherapeutic efficacy [28] [3] [29] [26]. On the other hand, ferroptotic damage could contribute to inflammation-related immunosuppression within the tumour microenvironment and promotes the growth of tumors [27] [30]. The role of ferroptosis in lung adenocarcinoma has not been elaborated. Our research provides a new perspective for the development of lung adenocarcinoma.

Ferroptosis was once considered as a novel cell death process which was distinct from apoptosis, necrosis, and autophagy [4]. However, studies from autophagy-deficient cells suggested that ferroptosis was a type of autophagy-dependent cell death in some conditions [8]. Autophagy, especially certain types of selective autophagy, such as ferritinophagy [31] [32], lipophagy [33], clockophagy [34] [35], and chaperone-mediated autophagy [34], could promote ferroptosis through lipid peroxidation.

FANCD2 (FA complementation group D2) contributes heterogeneously to Fanconi anemia (FA), a genetic disorder characterized by birth defects, progressive bone marrow failure, and cancer-prone phenotype [36]. The patients with aberranct expression of FANCD2 possess abnormality in chromosomal breakage and hypersensitivity to DNA crosslinking agents [37]. As an DNA damage response regulator, FANCD2 also can regulate ferroptosis sensitivity by inhibiting iron accumulation and lipid peroxidation in an autophagy-independent manner [38] [39]. FANCD2 has an intricate relationship with tumor. The heterozygous and somatic mutations of FANCD2 were reported in a variety of malignancies, including pancreatic cancers and squamous cell carcinomas [40] [41]. The overexpression of FANCD2 was involved in metastasis-prone melanomas [42] and colorectal cancer [43]. In our study, FANCD2 was identified as an autophagy-dependent ferroptosis-related key gene in the LUAD occrrence after comprehensive analysis.

In tumor microenvironment, immune cells could regulate tumour ferroptosis during cancer immunotherapy [3]. Besides, ferroptosis also could regulate immunity activity within the tumour microenvironment [30]. The potential connection between behavior of immune cells in the tumor microenvironment and ferroptosis needs to be further studied. In our study, the high expression of FANCD2 group achieved a high fraction of neutrophil, which revealed that ferroptosis-related gene FANCD2 may be closely associated with neutrophil-mediated tumor immunity.

In accordance with above findings, the contents of the antigen processing and presentation were enriched by KEGG analyses. In adaptive immunity, neutrophils play a significant role in internalizing antigen and regulating antigen-specific responses [44]. When ferroptosis occurred, the immunogenic signals, such as lipid mediators, were released by the death cells. Subsequently, the antigen-presenting cells including neutrophils were attracted to the site of ferroptotical cells [30]. A multitude of recuited neutrophils further activated the immune system to resist the invasion of pathogenic factors. Abnormal and uncotrolled ferroptosis may be implicated with invalid inmmunity [30]. Our research indicated that high expression of FANCD2 induced the aberrent ferroptosis and further contributed to the abnormality of anti-tumor immunity in patients with LUAD.

TMB level has demonstrated utility in selecting patients for response to immunetherapy and has proven to be an important biomarker for patient selection. Patients who are in high TMB benefit more from immunotherapy, which provided a new avenue to make LUAD treatment more precise [45]. In our study, the LUAD patients with a high expression level of FANCD2 achieved a high TMB, indicating that these patients may gain more benefit from immunotherapy than those with a low FANCD2 expression level. Among the mutation genes, tumor suppressor gene inactivation, such as P53, is very common in LUAD

[46]. P53 activation has been explored to be essential in some other activities to suppress tumor progression [47] [48], whereas the anti-P53 activity traditionally drives cell senescence, cell cycle arrest and apoptosis [49]. Additionally, P53 was reported to be correlated with ferroptosis, and it could inhibit cystine uptake and sensitize cells to ferroptosis. Study revealed that the sensitivity of ROS-induced ferroptosis was markedly increased in P53-activated cells [50]. Our study founds that P53 is the most frequently mutated gene and positively correlated with a higher FANCD2 expression level, which indicated that the P53 mutation may activate the FANCD2-mediated ferroptosis and increase the response of immunotherapy in LUAD.

Conclusions

Our study identified a novel autophagy-dependent ferroptosis-related gene, FANCD2 gene which was proved to be independently associated with OS in LUAD and may serve as prognostic factor for LUAD. FANCD2 expression level was negatively correlated with immune infiltrating levels but positively correlated with somatic mutation in LUAD, which indicated that FANCD2 may act as a potential inhibitor to interfere with immune cells and revealed the potential relationship and interaction between ferroptosis and immunity in LUAD pathogenesis. More mechanistic studies are needed to verify the role and function of FANCD2-mediated feroptosis in the LUAD in future.

Abbreviations

LUAD, lung adenocarcinoma; TMB, tumor mutation burden; TCGA, The Cancer Genome Atlas; GEO, Gene Expression Omnibus; DEGs, Differentially expressed genes; OS, overall survival; K-M, Kaplan-Meier; ROC, receiver operating characteristic; GO, Gene ontology; KEGG, Kyoto encyclopedia of genes and genomes; TIMER, Tumor Immune Estimation Resource; HGNC, HUGO Gene Nomenclature Committee; FDR, false discovery rate; GEPIA, Gene Expression Profiling Interactive Analysis; HPA, The Human Protein Atlas database; IC50, The half maximal inhibitory concentration; ssGSEA, Single Sample Gene Set Enrichment Analysis; SNV, single-nucleotide variant; mRNA, messenger RNA; FANCD2, FA Complementation Group D2; SNP, single nucleotide polymorphism; INS, insertion; DEL, deletion.

Declarations

Conflict of Interest

No authors report any conflict of interest.

Funding

This work was supported by the “National Natural Science Foundation of China (81871986)”.

Author Contributions

Huikai Miao and Qiannan Ren conceived and designed the study. Dongni Chen, Hongmu Li and Mingyue Zeng performed the analysis, prepared the figures and tables and wrote the main manuscript. Youfang Chen and Zhesheng Wen were involved in critically revising the manuscript. All authors read and approved the final manuscript.

Ethics approval and consent to participate

The clinical tissue samples of LUAD were obtained from patients who received surgery in Thoracic Oncology Department of Sun Yat-sen University Cancer Center, which was approved by the Institutional Review Committee of Sun Yat-sen University Cancer Center.

Data Availability

The data used to support the findings of this study are available from the corresponding author upon request.

Acknowledgements

We thank all patients who provide their tissue sample in this study.

Consent for publication

All authors agree to the publication of our work entitled “Comprehensive analysis of the autophagy-dependent ferroptosis-related gene FANCD2 in lung adenocarcinoma” to Journal of Experimental & Clinical Cancer Research.

References

1. Siegel RL, Miller KD, Jemal A. Cancer statistics, 2020. CA Cancer J Clin. 2020;70(1):7–30.
2. Siegel RL, Miller KD, Jemal A. Cancer statistics, 2019. CA Cancer J Clin. 2019;69(1):7–34.
3. Wang W, et al. CD8(+) T cells regulate tumour ferroptosis during cancer immunotherapy. Nature. 2019;569(7755):270–4.
4. Dixon SJ, et al. Ferroptosis: an iron-dependent form of nonapoptotic cell death. Cell. 2012;149(5):1060–72.
5. Stockwell BR, et al. Ferroptosis: A Regulated Cell Death Nexus Linking Metabolism, Redox Biology, and Disease. Cell. 2017;171(2):273–85.
6. Tang D, et al. The molecular machinery of regulated cell death. Cell Res. 2019;29(5):347–64.
7. Xie Y, et al. Ferroptosis: process and function. Cell Death Differ. 2016;23(3):369–79.
8. Zhou B, et al. Ferroptosis is a type of autophagy-dependent cell death. Semin Cancer Biol. 2020;66:89–100.
9. Wang Y, et al., *Iron Metabolism in Cancer*. Int J Mol Sci, 2018. 20(1).

10. Ganz T, Nemeth E. Iron homeostasis in host defence and inflammation. Nat Rev Immunol. 2015;15(8):500–10.
11. Zhang F, et al. Engineering Magnetosomes for Ferroptosis/Immunomodulation Synergism in Cancer. ACS Nano. 2019;13(5):5662–73.
12. Alexandrov LB, et al. Signatures of mutational processes in human cancer. Nature. 2013;500(7463):415–21.
13. Van Allen EM, et al. Whole-exome sequencing and clinical interpretation of formalin-fixed, paraffin-embedded tumor samples to guide precision cancer medicine. Nat Med. 2014;20(6):682–8.
14. Chalmers ZR, et al. Analysis of 100,000 human cancer genomes reveals the landscape of tumor mutational burden. Genome Med. 2017;9(1):34.
15. Schumacher TN, Kesmir C, van Buuren MM. *Biomarkers in cancer immunotherapy* Cancer Cell. 2015;27(1):12–4.
16. Rhodes DR, et al. Oncomine 3.0: genes, pathways, and networks in a collection of 18,000 cancer gene expression profiles. Neoplasia. 2007;9(2):166–80.
17. Tang Z, et al. GEPIA: a web server for cancer and normal gene expression profiling and interactive analyses. Nucleic Acids Res. 2017;45(W1):W98–102.
18. Colwill K, Working GRenewablePBinder, Graslund S. A roadmap to generate renewable protein binders to the human proteome. Nat Methods. 2011;8(7):551–8.
19. Duma N, Santana-Davila R, Molina JR. Non-Small Cell Lung Cancer: Epidemiology, Screening, Diagnosis, and Treatment. Mayo Clin Proc. 2019;94(8):1623–40.
20. Geeleher P, Cox N, Huang RS. pRRophetic: an R package for prediction of clinical chemotherapeutic response from tumor gene expression levels. PLoS One. 2014;9(9):e107468.
21. Li T, et al. TIMER: A Web Server for Comprehensive Analysis of Tumor-Infiltrating Immune Cells. Cancer Res. 2017;77(21):e108–10.
22. Lin F, Chen Z. Standardization of diagnostic immunohistochemistry: literature review and geisinger experience. Arch Pathol Lab Med. 2014;138(12):1564–77.
23. Remark R, et al. The non-small cell lung cancer immune contexture. A major determinant of tumor characteristics and patient outcome. Am J Respir Crit Care Med. 2015;191(4):377–90.
24. Pfeifhofer-Obermair C, et al. Iron in the Tumor Microenvironment-Connecting the Dots. Front Oncol. 2018;8:549.
25. Thanan R, et al. Inflammation-induced protein carbonylation contributes to poor prognosis for cholangiocarcinoma. Free Radic Biol Med. 2012;52(8):1465–72.
26. Jiang M, et al. Targeting ferroptosis for cancer therapy: exploring novel strategies from its mechanisms and role in cancers. Transl Lung Cancer Res. 2020;9(4):1569–84.
27. Chen X, et al. Broadening horizons: the role of ferroptosis in cancer. Nat Rev Clin Oncol. 2021;18(5):280–96.

28. Viswanathan VS, et al. Dependency of a therapy-resistant state of cancer cells on a lipid peroxidase pathway. Nature. 2017;547(7664):453–7.
29. Zheng DW, et al. Switching Apoptosis to Ferroptosis: Metal-Organic Network for High-Efficiency Anticancer Therapy. Nano Lett. 2017;17(1):284–91.
30. Friedmann Angeli JP, Krysko DV, Conrad M. Ferroptosis at the crossroads of cancer-acquired drug resistance and immune evasion. Nat Rev Cancer. 2019;19(7):405–14.
31. Gao M, et al. Ferroptosis is an autophagic cell death process. Cell Res. 2016;26(9):1021–32.
32. Hou W, et al. Autophagy promotes ferroptosis by degradation of ferritin. Autophagy. 2016;12(8):1425–8.
33. Bai Y, et al. Lipid storage and lipophagy regulates ferroptosis. Biochem Biophys Res Commun. 2019;508(4):997–1003.
34. Yang MH, et al., *Clockophagy is a novel selective autophagy process favoring ferroptosis*. Science Advances, 2019. 5(7).
35. Liu J, et al. Autophagic degradation of the circadian clock regulator promotes ferroptosis. Autophagy. 2019;15(11):2033–5.
36. Longerich S, et al. Stress and DNA repair biology of the Fanconi anemia pathway. Blood. 2014;124(18):2812–9.
37. Timmers C, et al. Positional cloning of a novel Fanconi anemia gene, FANCD2. Mol Cell. 2001;7(2):241–8.
38. Song X, et al. FANCD2 protects against bone marrow injury from ferroptosis. Biochem Biophys Res Commun. 2016;480(3):443–9.
39. Sertorio M, et al., *Fancd2 Deficiency Impairs Autophagy Via Deregulating The Ampk/Foxo3a/Akt Pathway*. Blood, 2013. 122(21).
40. van der Heijden MS, et al. Fanconi anemia gene mutations in young-onset pancreatic cancer. Cancer Res. 2003;63(10):2585–8.
41. Wreesmann VB, et al. Downregulation of Fanconi anemia genes in sporadic head and neck squamous cell carcinoma. ORL J Otorhinolaryngol Relat Spec. 2007;69(4):218–25.
42. Kauffmann A, et al. High expression of DNA repair pathways is associated with metastasis in melanoma patients. Oncogene. 2008;27(5):565–73.
43. Ozawa H, et al. FANCD2 mRNA overexpression is a bona fide indicator of lymph node metastasis in human colorectal cancer. Ann Surg Oncol. 2010;17(9):2341–8.
44. Vono M, et al. Neutrophils acquire the capacity for antigen presentation to memory CD4(+) T cells in vitro and ex vivo. Blood. 2017;129(14):1991–2001.
45. Chan TA, et al. Development of tumor mutation burden as an immunotherapy biomarker: utility for the oncology clinic. Ann Oncol. 2019;30(1):44–56.
46. Berkers CR, et al. Metabolic Regulation by p53 Family Members. Cell Metab. 2013;18(5):617–33.

47. Valente LJ, et al. *p*53 efficiently suppresses tumor development in the complete absence of its cell-cycle inhibitory and proapoptotic effectors p21, Puma, and Noxa. Cell Rep. 2013;3(5):1339–45.
48. Brady CA, et al. Distinct p53 transcriptional programs dictate acute DNA-damage responses and tumor suppression. Cell. 2011;145(4):571–83.
49. Brooks CL, Gu W. Ubiquitination, phosphorylation and acetylation: the molecular basis for p53 regulation. Curr Opin Cell Biol. 2003;15(2):164–71.
50. Jiang L, et al. Ferroptosis as a p53-mediated activity during tumour suppression. Nature. 2015;520(7545):57–62.

Figures

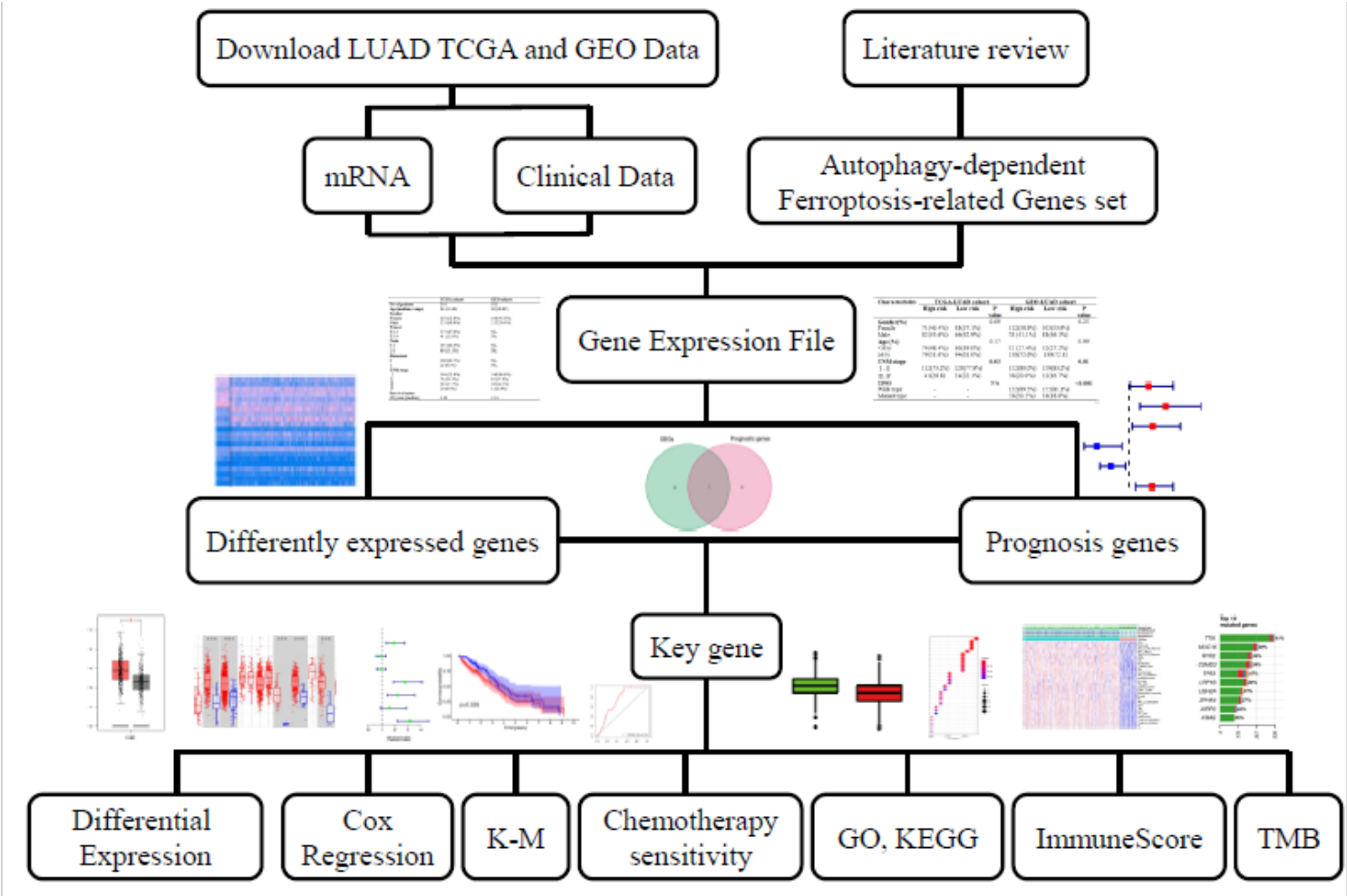

Figure 1

Research framework for the exploration procedure and comprehensive analysis of the autophagy-dependent ferroptosis-related gene. LUAD, Adenocarcinoma of lung; TCGA, The Cancer Genome Atlas; GEO, Gene Expression Omnibus; mRNA, messenger RNA; K-M, Kaplan-Meier; GO, Gene Ontology; KEGG, Kyoto Encyclopedia of Genes and Genomes; TMB, Tumor Mutational Burden.

Autophagy-dependent ferroptosis-related gene sets

Ferritinophagy	Lipophagy	Clockophagy	Chaperone-mediated autophagy	Unknown	
AMPK	AGER	ARNTL	GPX4	15LO1	HMGB1
ATG7	ATG5	BMAL1	HSP90	ACSL4	HSPA5
ATPR	BECN1	EGLN2	LGMN	ATG13	HSPB1
FTH1	CPT1A	FIN56	RIPK1	ATG16L1	HUR
IREB2	KRAS	HIF1A		ATG3	LONP1
IRP2	RAB27A	P62		ATG4B	NFE2L2
mTOR	RAB7A	RNTL		BECLIN1	NOX4
NCOA4	RSL3	RSL3		CDC4	NRF2
NRF2	SLC7A11	SQSTM1		CGAS	P53
p70S6k	STAT3			CISD1	PEBP1
ZFP36	STING1			COPZ1	PI3K
	TMEM173			ELAVL1	PIRIN
	TPD52			FANCD2	POLG
				FBXW7	PP2A
				FTY720	SFSGLPS
				HERC2	SIRT3
					SLC40A1

Figure 2

Autophagy-dependent ferroptosis-related genes.

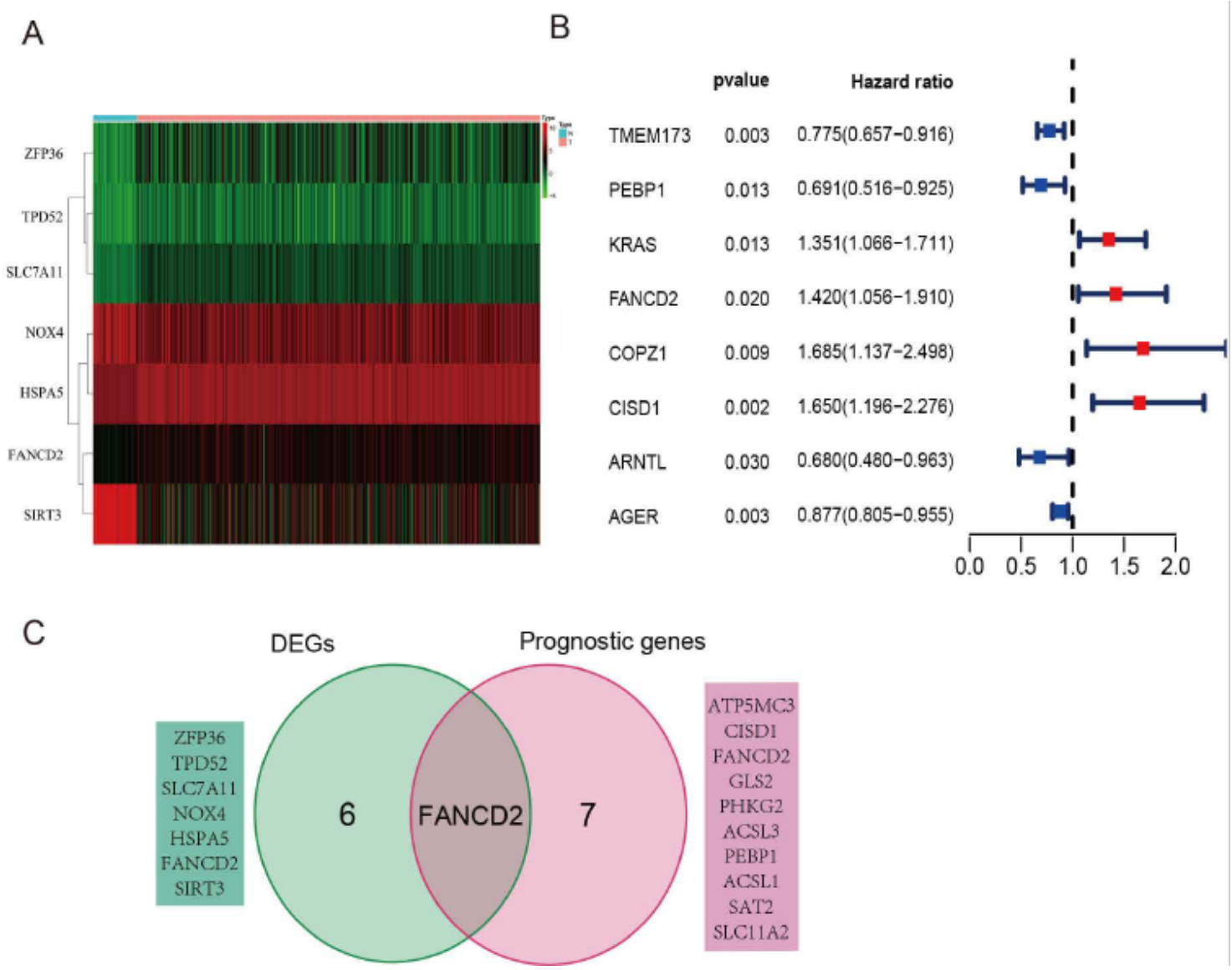

Figure 3

Identification of the candidate autophagy-dependent ferroptosis-related genes in the TCGA cohort. (A) There are 7 genes which were differential expressed between normal and lung tumor tissue. (B) Forest plots showing the results of the univariate Cox regression analysis between gene expression and OS. (C) Venn diagram to identify differentially expressed genes between tumor and adjacent normal tissue that were correlated with OS. TCGA, The Cancer Genome Atlas; OS, Overall Survival; DEGs, Differentially Expressed Genes.

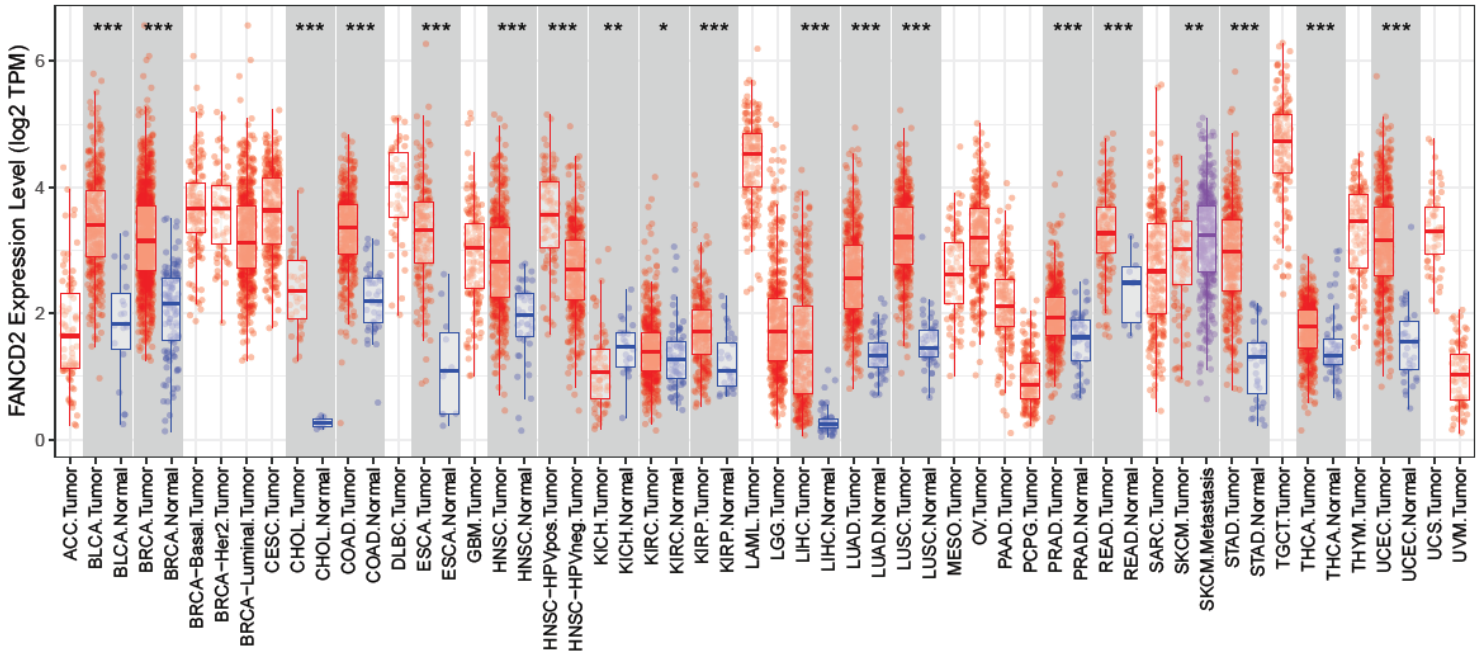

Figure 4

The transcription levels of FANCD2 in different types of cancers. FANCD2, FA Complementation Group D2.

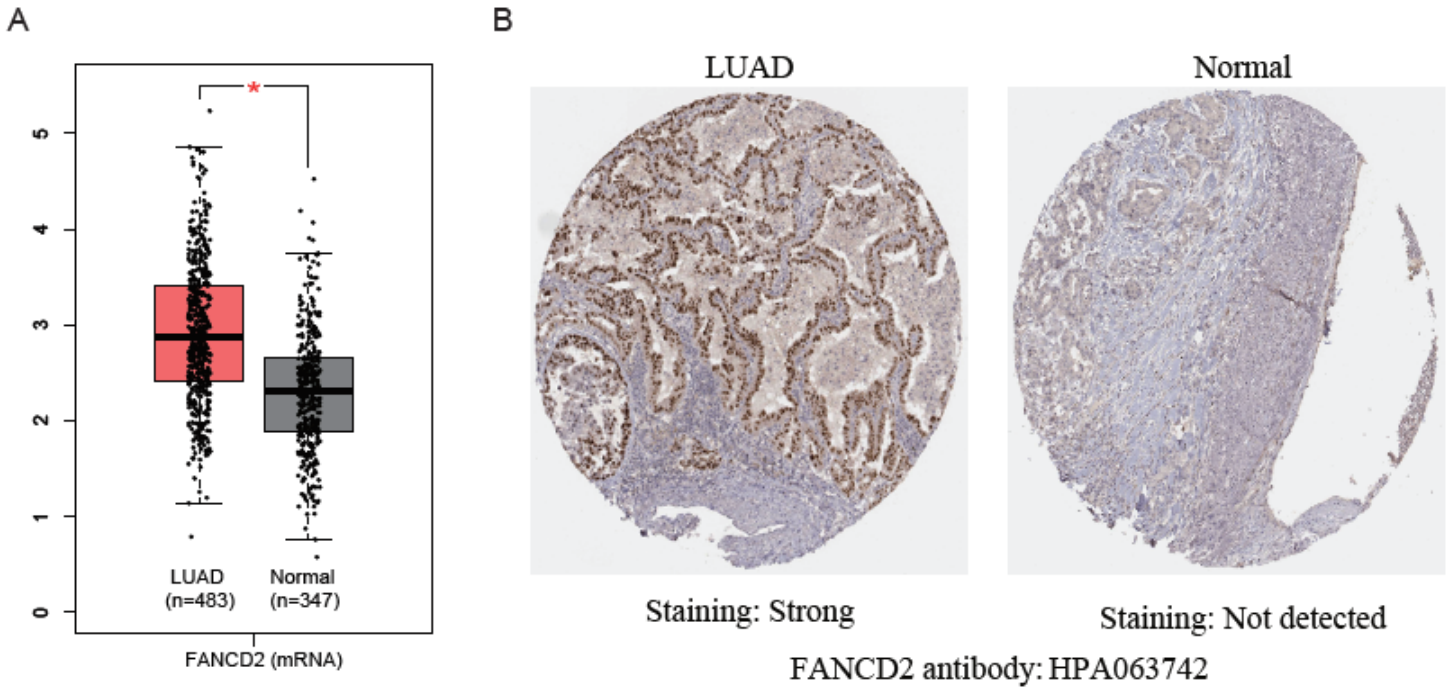

Figure 5

The expression levels of FANCD2 in LUAD. (A) The mRNA expression level of LUAD in GEPIA database. (B) The protein expression level of LUAD in HPA database. LUAD, Adenocarcinoma of lung; GEPIA, Gene

Expression Profiling Interactive Analysis; HPA, The Human Protein Atls; N, the number of tumors and normal tissues.

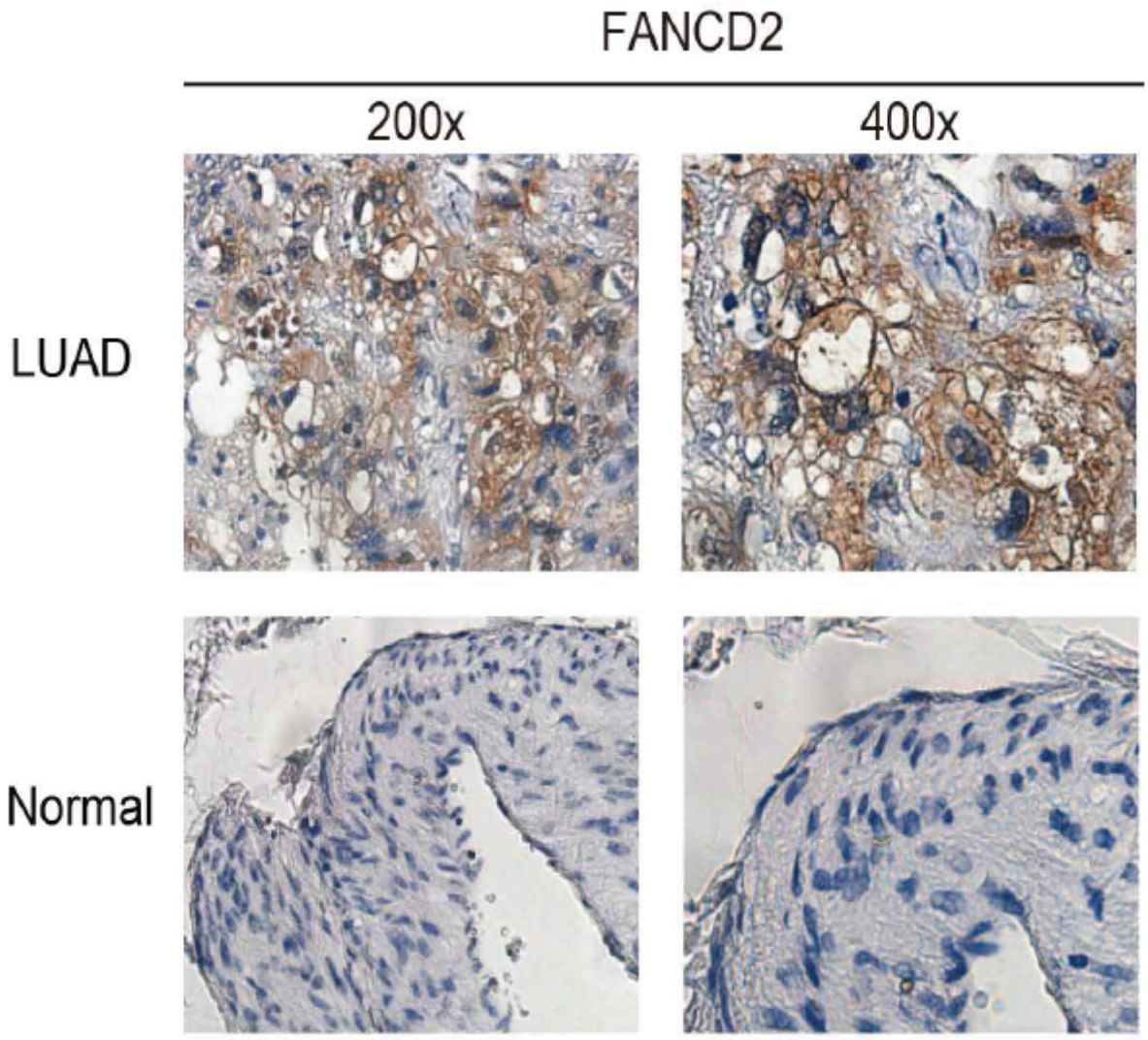

Figure 6

The protein expression levels of FANCD2 in LUAD patients by immunohistochemistry. LUAD, Adenocarcinoma of lung;

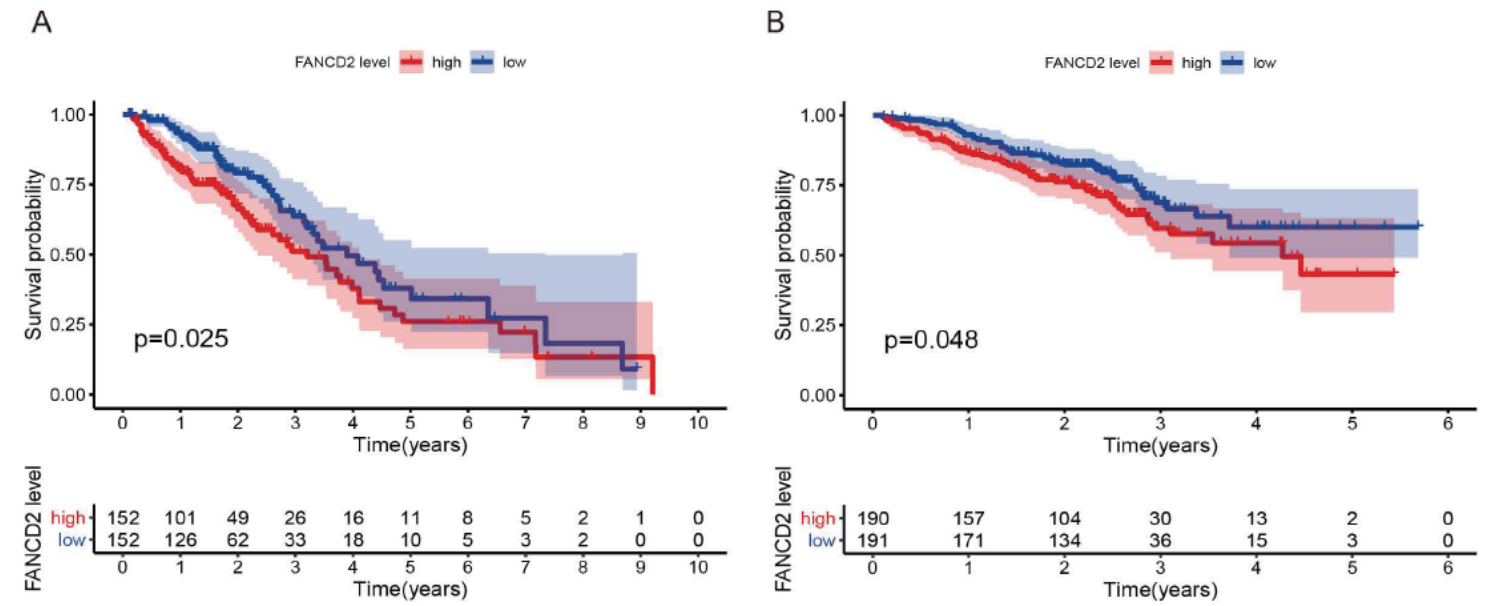

Figure 7

Survival analysis of FANCD2 in LUAD in TCGA database (A) and GEO cohort (B). LUAD, Adenocarcinoma of lung; TCGA, The Cancer Genome Atlas; GEO, Gene Expression Omnibus;

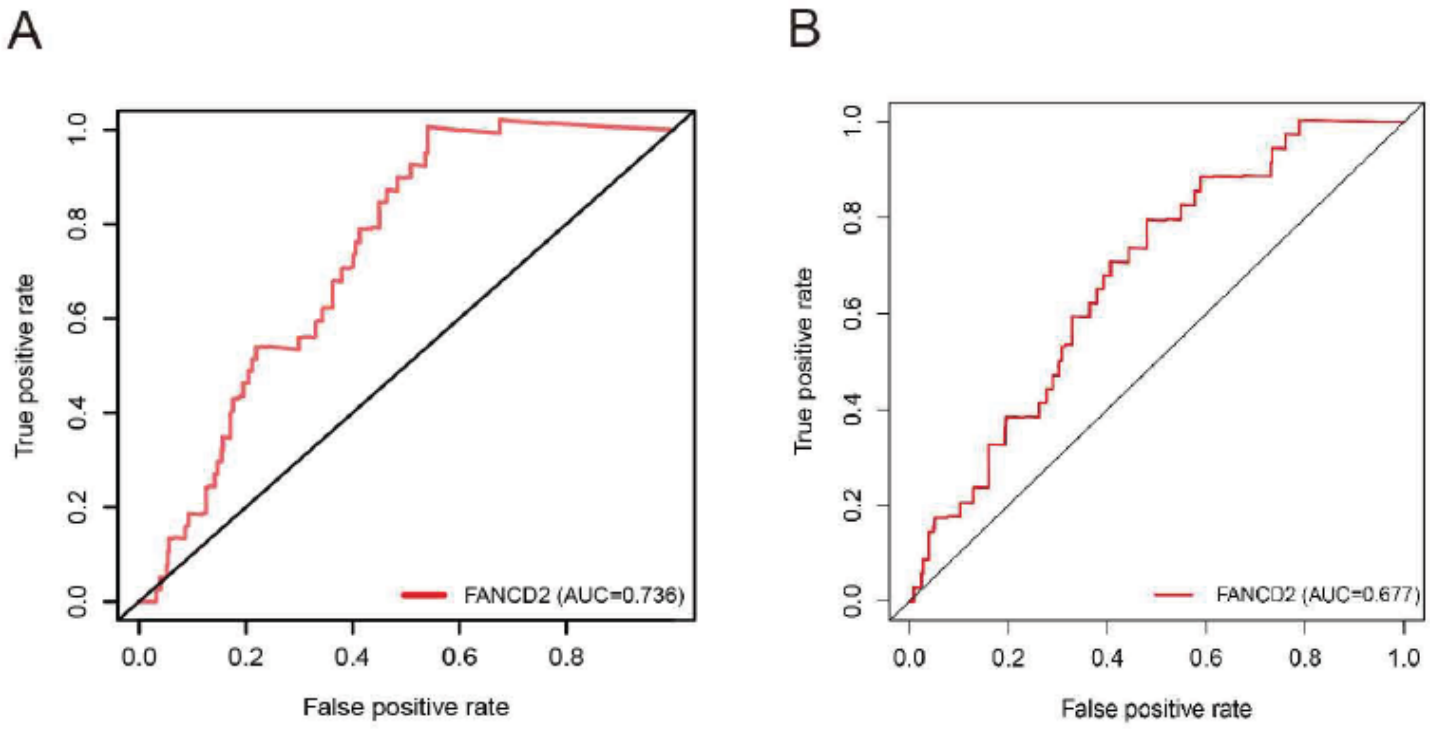

Figure 8

ROC curve of the FANCD2 risk score. The risk score is shown by the receiver operating characteristic curve for predicting survival of the TCGA cohort (A) and the GEO cohort (B). ROC curve, receiver operating characteristic curve; TCGA, The Cancer Genome Atlas; GEO, Gene Expression Omnibus.

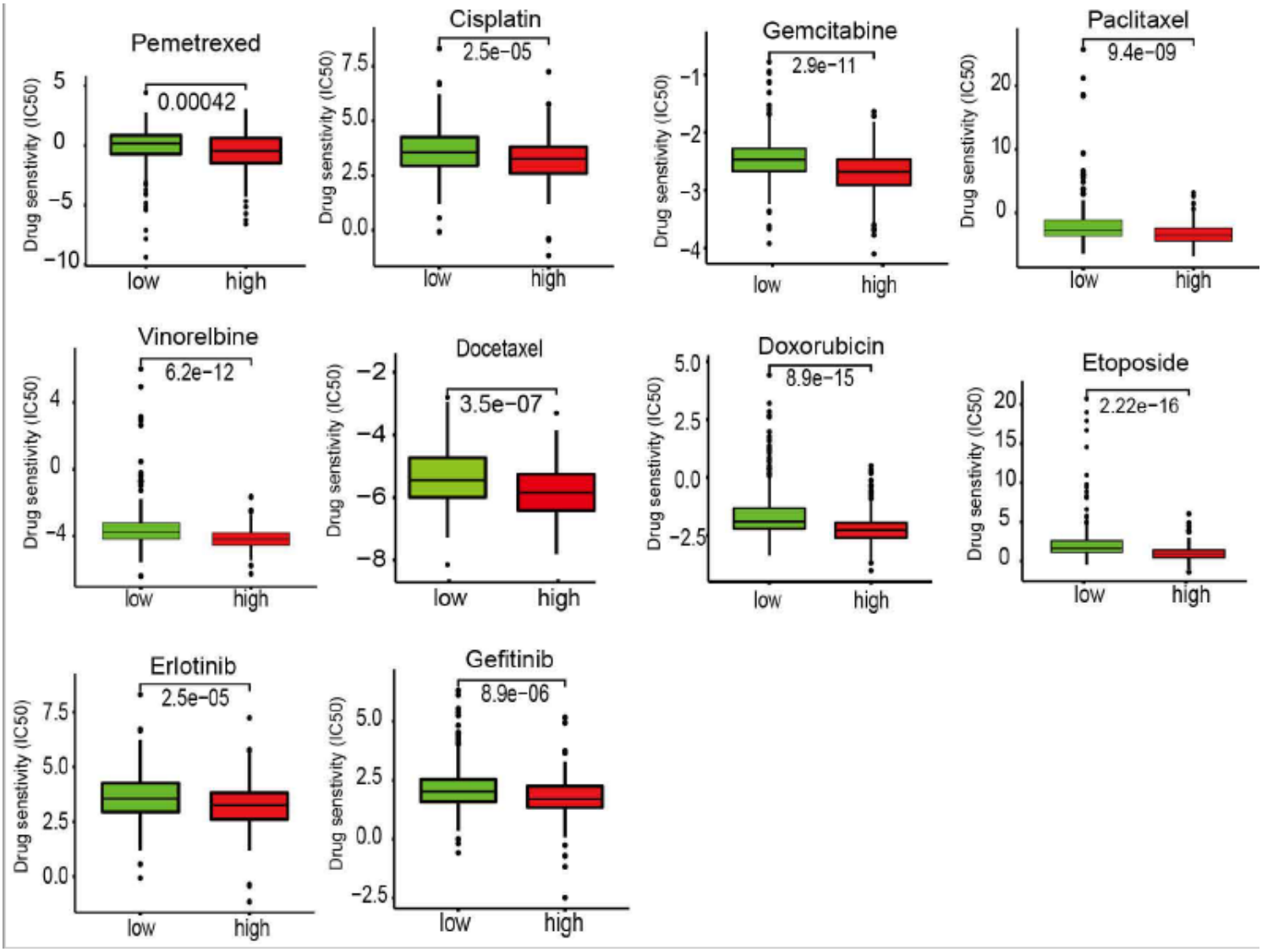

Figure 9

Chemotherapeutic responses in high- and low-risk patients with LUAD.

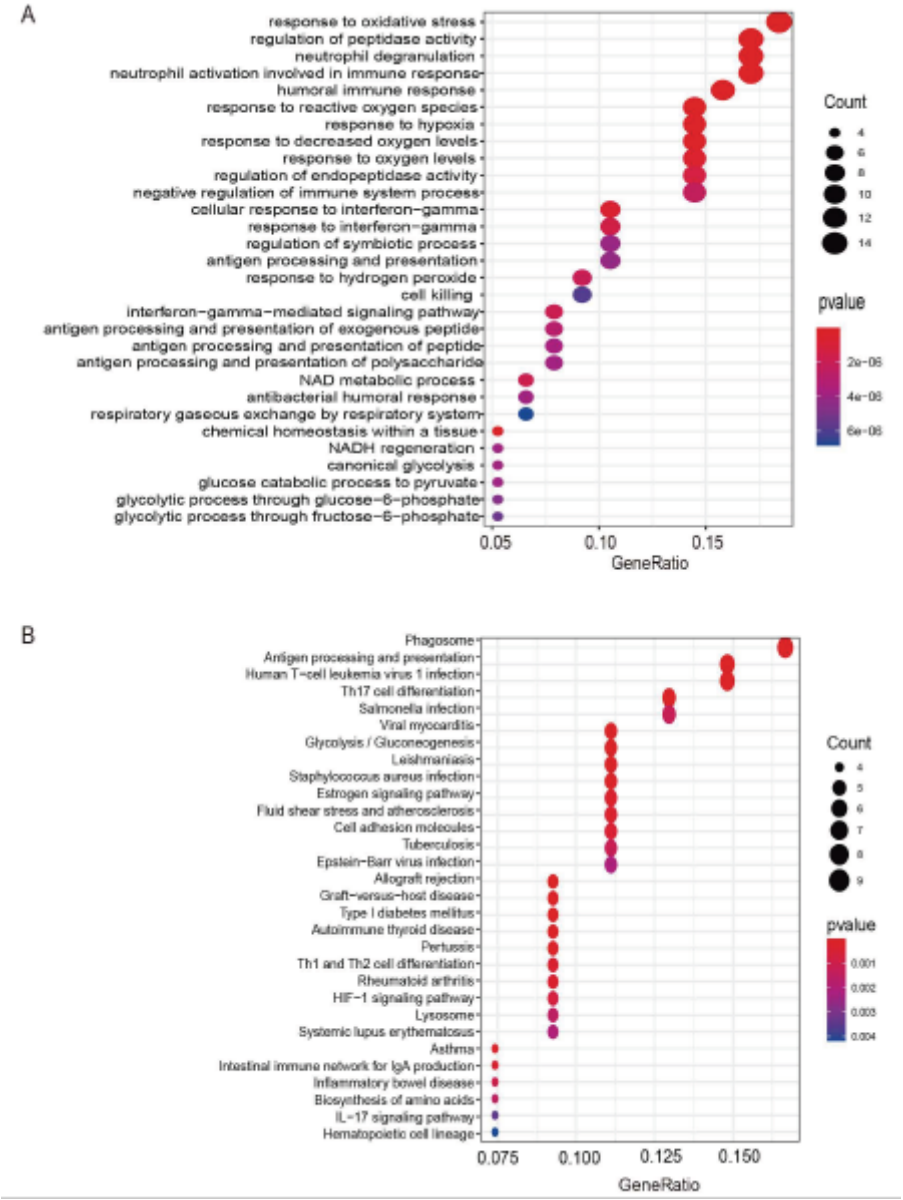

Figure 10

Representative results of GO (A) and KEGG analyses (B). GO, Gene Ontology; KEGG, Kyoto Encyclopedia of Genes and Genomes.

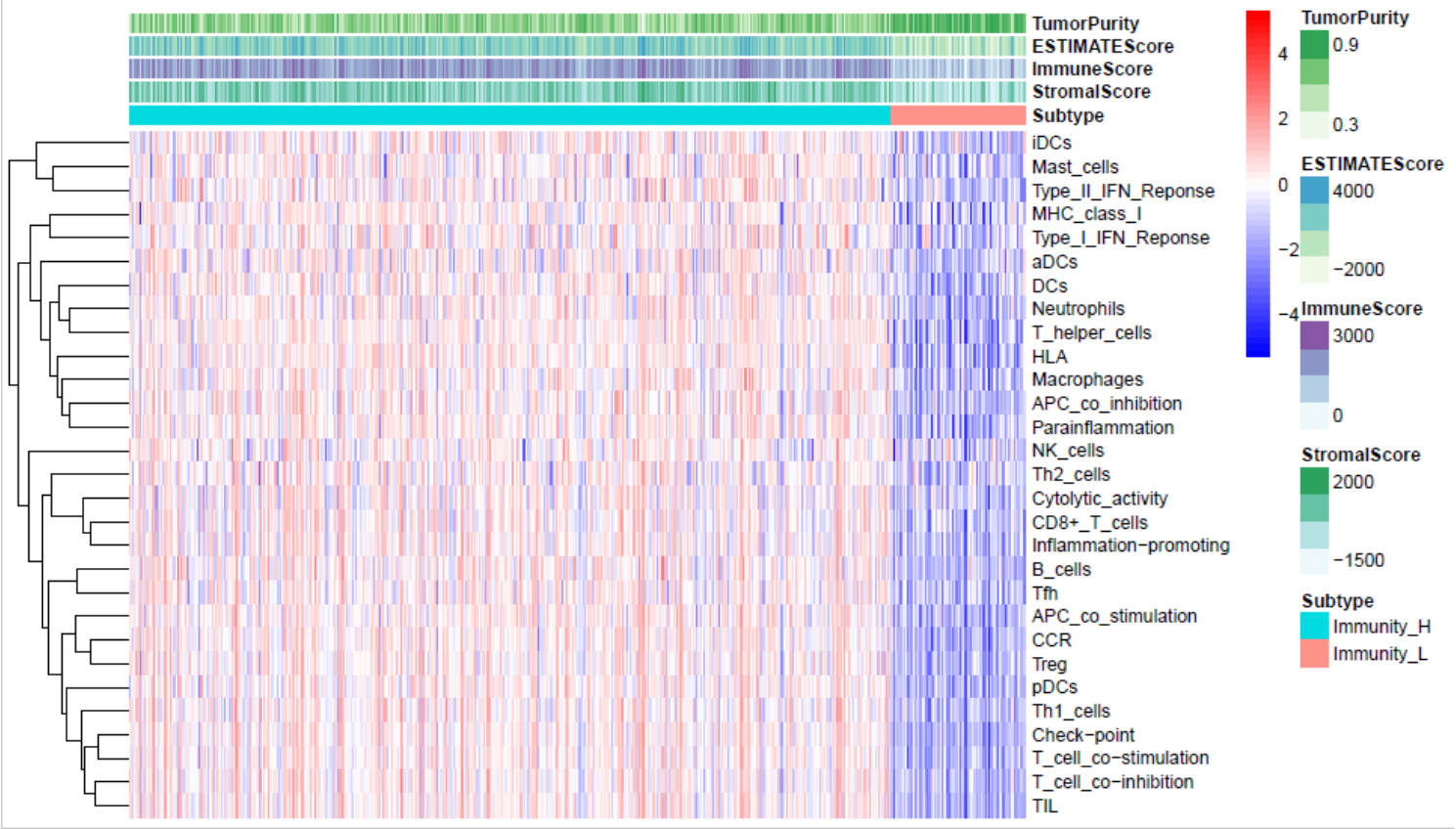

Figure 11

The enrichment levels of immune-related process and immune score in the LUAD cohort.

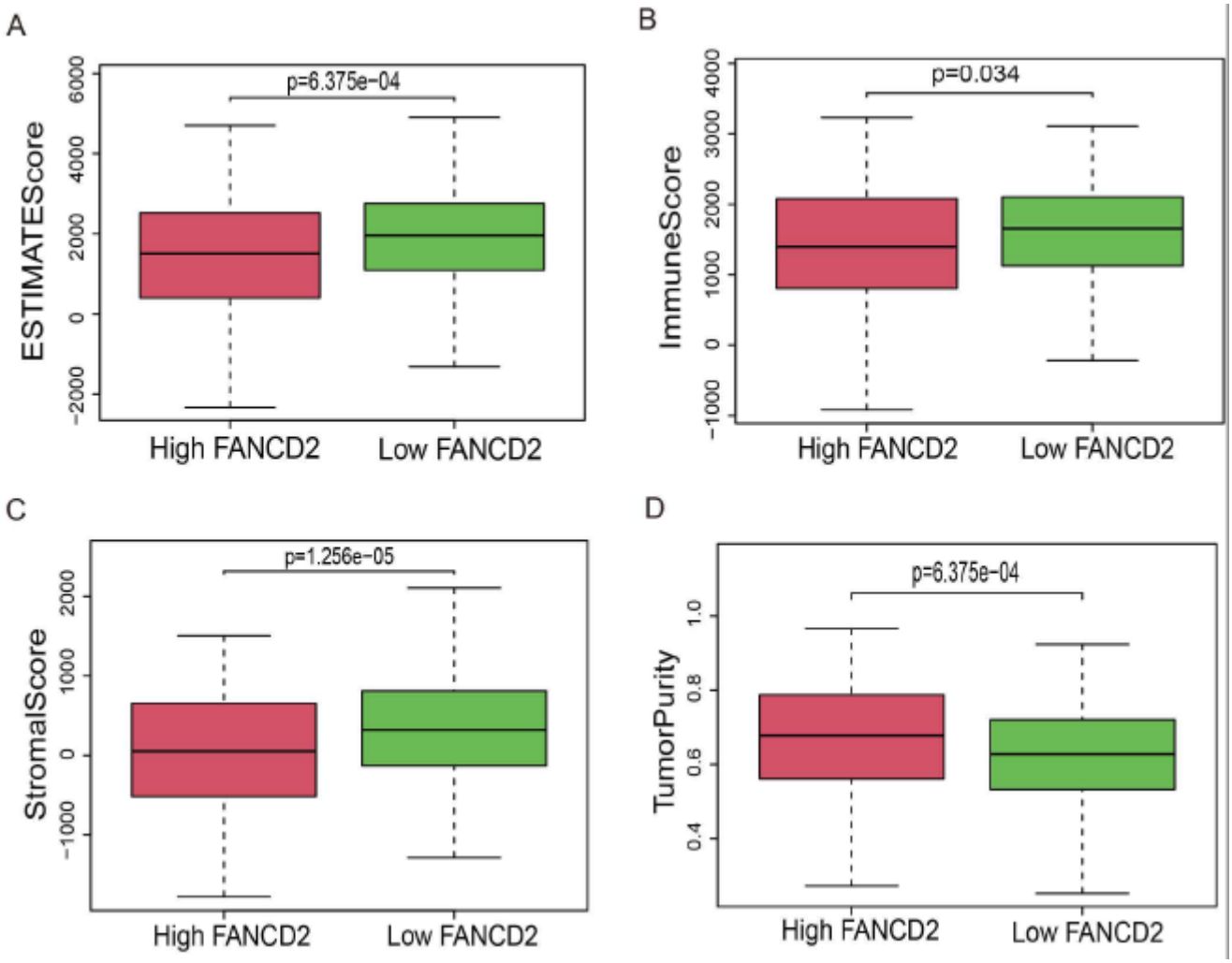

Figure 12

The correlation between the FANCD2 expression level and ESTIMATE Score (A), Immune Score (B), Stromal Score (C), Tumor Purity (D).

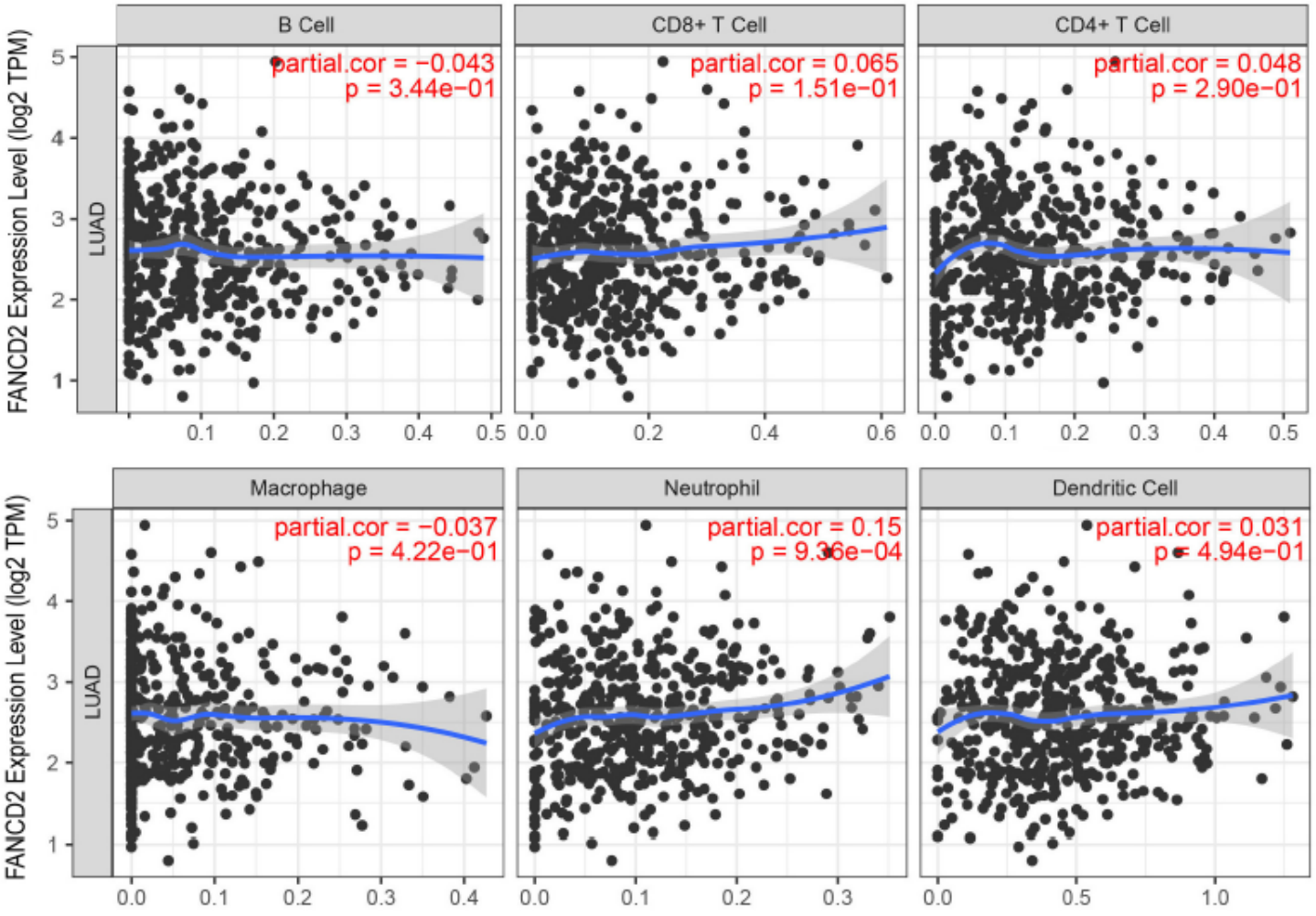

Figure 13

The correlation between the FANCD2 expression level and six immune cells infiltration level.

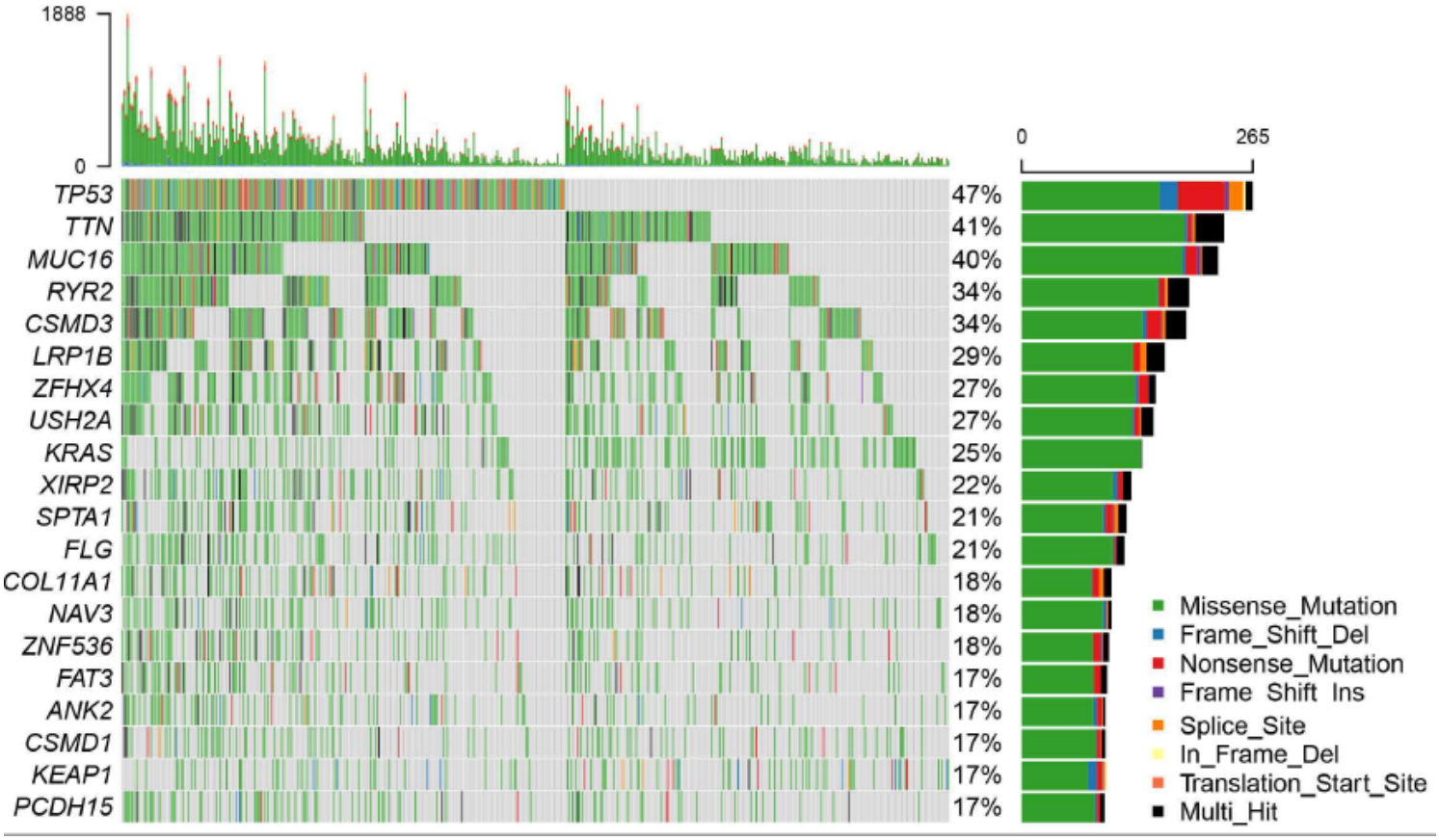

Figure 14

The oncoplot of the TMB. TMB, tumor mutational burden.

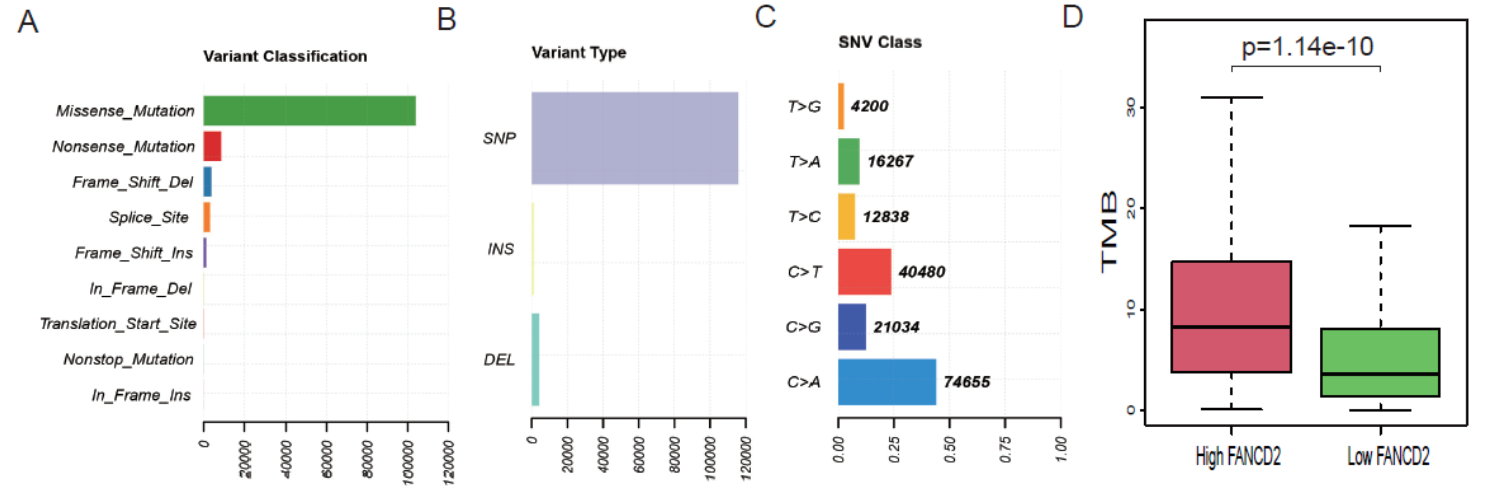

Figure 15

The Variant Classification (A), the Variant Type (B), the Single Nucleotide Variant Class (C), the correlation of the FANCD2 expression level and TMB (D) in the LUAD cohort. SNP, single nucleotide polymorphism; INS, insertion; DEL, deletion; SNV, single nucleotide variants; TMB, tumor mutational burden.